

# **ScienceDirect**



IFAC PapersOnLine 56-3 (2023) 241-246

# Synchronization of a pair of nonholonomic oscillators

Ali Mohseni \* Phanindra Tallapragada \*

\* Department of Mechanical Engineering, Clemson University, Clemson, SC 29634 USA (e-mail: mohseni@g.clemson.edu, ptallap@clemson.edu).

Abstract: The paper introduces the novel problem of the synchronization of a pair of identical mobile nonholonomic oscillators, the so-called Chaplygin sleighs, moving on a movable platform with springs. Each Chaplygin sleigh is actuated by a periodic torques of the same amplitude and frequency, resulting in a limit cycle in a reduced velocity space. The frictional constraint forces couple the motion of the two Chaplygin sleighs and the platform. The limit cycles of the coupled oscillators are dependent on the relative phase of actuation on the sleighs. We show that the coupled limit cycles become identical but with anti-phase synchronization, where the amplitude and frequency of oscillations and the average translational speeds of the two sleighs become equal. Moreover, in such anti-phase synchronization, the heading angle of both sleighs converge, producing motion in a formation.

Copyright © 2023 The Authors. This is an open access article under the CC BY-NC-ND license (https://creativecommons.org/licenses/by-nc-nd/4.0/)

Keywords: Nonholonomic systems, Coupled Nonholonomic Oscillators, Synchronization.

### 1. INTRODUCTION

This paper revisits the problem of synchronization of two coupled oscillators, but with the novelty that the oscillators are mobile nonholonomic systems moving on a platform. Their motion is coupled through their interaction with a movable platform with springs. The problem of synchronization of two coupled pendulum oscillators goes back to Huygens' (Huygens (1669)) observation on the (anti)synchronization of two pendulum clocks that are weakly coupled by a beam, where he observed that two identical pendulum oscillators hung on a beam synchronized in about 30 minutes with the same amplitude and frequency but were out of phase, see Bennett et al. (2002); Willms et al. (2017) for a historical review. Synchronization of large collections of oscillators has seen an explosion of interest with Winfree's observation (in Winfree (1967)) of phase transition like behavior in coupled oscillators underlying circadian rhythms and Kuramoto's explanation using an approximate model (in Kuramoto (1975)). The synchronization of coupled oscillators is a fundamental concept in nonlinear science; see for example Pikovsky et al. (2001) and Strogatz (2003). More recent motivation for the study of synchronization has been from the area of collective animal locomotion, see for example Buhl et al. (2006); Bialek et al. (2012); Herbert-Read (2016) and associated applications in robotics.

The paper considers the motion of two identical Chaplygin sleighs on a platform. The Chaplygin sleigh is a well-known nonholonomic system where friction on the sleigh enforces a (no slip) nonholonomic constraint; see Neimark and Fufaev (1972) and Borisov and Mamaev (2009) for a review. Each Chaplygin sleigh is actuated by a periodic torques of the same amplitude and frequency, which can be imagined

as being applied due to the motion of an internal rotor. When the sleigh moves on a fixed surface with viscous damping, the periodic torque leads to a limit cycle in the velocity space, as described in Fedonyuk and Tallapragada (2018). When such an actuated Chaplygin sleigh is placed on a movable platform, the nonholonomic constraint (friction) force excites the motion of the platform. When two identical Chaplygin sleighs with periodic torques, thus possessing identical limit cycles in the velocity space, are placed on a movable platform, their dynamics and those of the platform are coupled. We show that depending on the phase difference between the actuating torques on the two sleighs, the individual limit cycles are modified. When the phase difference in the actuation is  $\pi$ , the limit cycles of the two oscillators become identical but are in anti-phase. In such anti-phase synchronization, the two Chaplygin sleighs move in the same average direction with the same speed. This heading direction is determined to be the average of the initial heading direction of the two sleighs.

The problem formulated in this paper and the results can be of significance in investigating the synchronization of the motion of robots coupled with the dynamics of the 'environment', such a millimeter scale robots moving on platforms or in pipes or fish-like swimming robots. The Chaplygin sleigh has in the past been used as a simplified model for a swimming robot, see for example the papers Pollard and Tallapragada (2017, 2019); Lee et al. (2019); Free et al. (2020). The results in this paper can lead to simplified models for the coordinated motion of hydrodynamically interacting swimmers. A related problem, that of the formation control of a collection of Chaplygin-sleigh like swimming robots, was described in Paley et al. (2021); Ghanem et al. (2020); however, the formation control was a result of feedback control, and the hydrodynamic interaction of two swimmers or the mechanical interaction

<sup>\*</sup> This work was supported by the NSF

of two sleighs were not modeled. The coupled dynamics of Chaplygin sleighs and a moving platform were investigated in Buchanan et al. (2020), but the anti phase synchronization of the limit cycles was not shown. To our knowledge, the current paper is the first where the synchronization of mobile nonholonomic oscillators is investigated and antiphase synchronization of limit cycles is demonstrated.

# 2. COUPLED NONHOLONOMIC OSCILLATOR MODEL

# 2.1 Review of Chaplygin sleigh dynamics

A schematic diagram of the Chaplygin sleigh is shown in Fig. 1. The sleigh has mass m and Point C shows the Center of mass. Its moment of inertia is I about point C. The point P represents the point of contact of the sharp knife edge or wheel with the ground. At this point (P), the sleigh can not slip in the transverse direction. The axes  $X_b$  and  $Y_b$  are body fixed where  $X_b$  is aligned with the line between P and the center of mass. The position of the center of mass of the sleigh is denoted by (x, y), and the orientation of the sleigh is  $\theta$ . The distance between P and the center of mass is b. The sleigh is imagined to carry a balanced rotor of the moment of inertia  $I_c$  at its center that is driven by a motor. If the relative angle that the rotor makes with the body axes is denoted by  $\phi$ , the motor exerts a torque  $\tau = -I_c \ddot{\phi}$  on the sleigh. The configuration manifold for the system, ignoring the internal shape variable  $\phi$ , is Q = SE2, parameterized by the (x,y) coordinates of the sleigh center of the mass and the angle  $\theta$  of the body axis with respect to the fixed spatial axis. The system is subject to the nonholonomic constraint (1),

$$-\sin\theta dx + \cos\theta dy - bd\theta = 0 \tag{1}$$

i.e. the transverse velocity (along the  $Y_b$  direction) of the point of contact P, be equal to zero. The velocity of P in the body frame is then  $u=\dot{x}\cos\theta+\dot{y}\sin\theta$ . The nonholonomic constraint is enforced by friction in the transverse direction at P. Beyond this friction, we further suppose that the motion of the sleigh is viscously damped with dissipation function  $D=\frac{1}{2}cu^2+\frac{1}{2}c_r\omega^2$ , where  $\omega=\dot{\theta}$ . The reduced equations of motion are then, see Fedonyuk and Tallapragada (2018)

$$\dot{u} = b\omega^2 - \frac{c}{m}u\tag{2}$$

$$\dot{\omega} = \frac{-mbu\omega}{I + mb^2} - \frac{c}{I + mb^2}\omega + \frac{\tau}{I + mb^2}$$
 (3)

### 2.2 A pair of Chaplygin sleighs on a platform

Now consider two identical Chaplygin sleighs placed on a platform of mass M which is connected by springs each of stiffness K to four walls as shown in fig. 2.

The spatial frame is denoted by  $X_S$  and  $Y_S$  and body frames on the sleighs are denoted by  $X_{b1} - Y_{b1}$  and  $X_{b2} - Y_{b2}$  respectively. The configuration manifold of the system is  $Q = SE2 \times SE2 \times \mathbb{R}^2$  parameterized by the generalized coordinates  $q = (X, Y, x_1, y_1, \theta_1, x_2, y_2, \theta_2)$ , where (X, Y) represent position of the center of the plate in

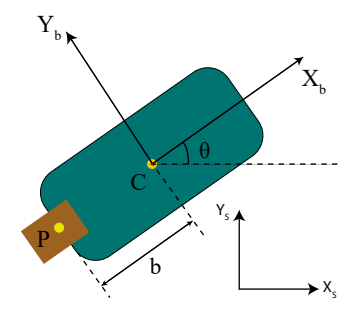


Fig. 1. The Chaplygin Sleigh. The body frame is denoted by axes  $X_b-Y_b$ . The point of contact, P, has zero velocity in  $Y_b$  direction

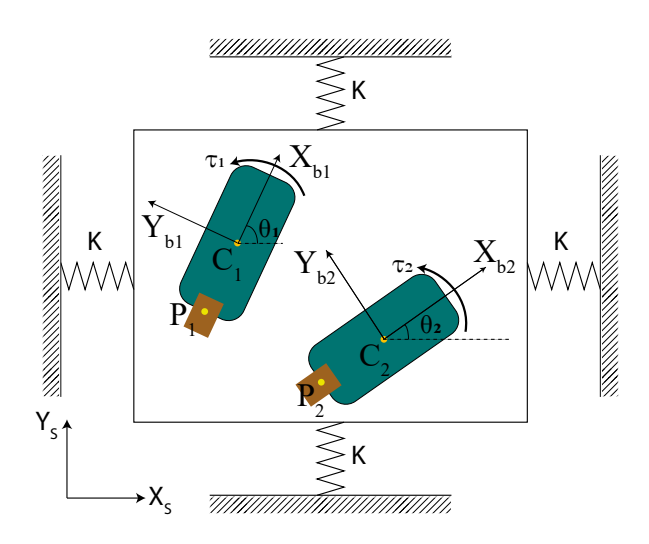


Fig. 2. System setup. Two similar actuated chaplygin sleigh on a spring supported horizontal plane.

the spatial frame and  $(x_i, y_i, \theta_i)$  for  $i \in [1, 2]$  represent the spatial position of the center of each sleigh and the angle made by the body  $X_{b_i}$ -axis with the spatial  $X_S$ -axis. The Lagrangian of the system is

$$\mathcal{L}(q, \dot{q}) = T - V$$

$$= \sum_{i=1}^{2} \left( \frac{1}{2} m [(\dot{X} + \dot{x}_{i})^{2} + (\dot{Y} + \dot{y}_{i})^{2}] + \frac{1}{2} I \dot{\theta_{i}}^{2} \right)$$

$$+ \frac{1}{2} M (\dot{X}^{2} + \dot{Y}^{2}) - \frac{1}{2} 2K X^{2} - \frac{1}{2} 2K Y^{2}$$
(4)

The two nonholonomic constraints are relative transverse velocity of  $P_i$  on each sleigh with respect to the platform should vanish. The two constraints are then

$$C_i(q, \dot{q}) = -\dot{x}_i \sin(\theta_i) + \dot{y}_i \cos(\theta_i) - b\dot{\theta}_i + \dot{X}\sin(\theta_i) - \dot{Y}\cos(\theta_i) = 0$$
(5)

We assume a Rayleigh Dissipation function on the sleighs as

$$D = \sum_{i=1}^{2} \left( \frac{1}{2} c u_i^2 + \frac{1}{2} c_r \dot{\theta}_i^2 \right)$$
 (6)

where  $u_i = \dot{x}_i \cos \theta_i + \dot{y}_i \sin \theta_i$  along the  $X_b$  axis. Then Rayleigh dissipation function can also be expressed as a

function of generalized coordinates and velocities:

$$D(q, \dot{q}) = \sum_{i=1}^{2} \frac{1}{2} c(\dot{x}_i \cos \theta_i + \dot{y}_i \sin \theta_i)^2 + \frac{1}{2} c_r \dot{\theta_i}^2$$
 (7)

The Euler-Lagrange equations are of the following form

$$\frac{d}{dt}\frac{\partial \mathcal{L}}{\partial \dot{q}^k} - \frac{\partial \mathcal{L}}{\partial q^k} = \sum_{i=1}^2 \lambda_i \frac{\partial C_i}{\partial \dot{q}^k} - \frac{\partial D}{\partial \dot{q}^k} + Q_k \tag{8}$$

with  $k \in [1,8]$ ,  $\lambda_i$  is the Lagrange multiplier associated with *i*th constraint, which in this setup is the friction force acting in the transverse directions at  $P_i$ (Point of contact of *i*th chaplygin seligh with the platform).  $Q_k$  is the generalized force. Straightforward calculation of the 8 for each k gives the equations of motion for this system as

$$M\ddot{X} + \sum_{i=1}^{2} m(\ddot{X} + \ddot{x}_i) + 2KX = \lambda_i \sin \theta_i$$
 (9)

$$M\ddot{Y} + \sum_{i=1}^{2} m(\ddot{Y} + \ddot{y}_i) + 2KY = -\lambda_i \cos \theta_i$$
 (10)

$$m(\ddot{X} + \ddot{x_i}) = -\lambda_i \sin(\theta_i) - c(\dot{x_i}\cos\theta_i + \dot{y_i}\sin\theta_i)\cos\theta_i$$
(11)

$$m(\ddot{Y} + \ddot{y}_i) = \lambda_i \cos(\theta_i) - c(\dot{x}_i \cos \theta_i + \dot{y}_i \sin \theta_i) \sin \theta_i$$
(12)

$$I\ddot{\theta_i} = -b\lambda_i - c_r\dot{\theta_i} + \tau_i \tag{13}$$

As a consequence of the nonholonomic constraints, a reduced number of equations can be used to describe the motion of the sleigh. This can be done by transforming the velocities into a body-fixed frame of reference. Further, the Lagrangian (4) is invariant with respect to translations in  $(x_i, y_i)$ , enabling a decoupling of the velocity equations of the Chaplygin sleigh with the group equations describing the evolution of the position of the Chaplygin sleighs. The velocity of the center of mass of the nth sleigh, can be expressed as  $v_n = u_n \hat{i}_b + b \hat{\theta}_n \hat{j}_b$  in the respective body frames. The velocity of each sleigh can be transformed to the spatial frame as

$$\dot{x}_i = \dot{X} + u_i \cos \theta_i - b\dot{\theta}_i \sin \theta_i \tag{14}$$

$$\dot{y}_i = \dot{Y} + u_i \sin \theta_i + b\dot{\theta}_i \cos \theta_i \tag{15}$$

and by diffrentiatin with respect to time the accelerations in the spatial frame can be obtained as

$$\ddot{x}_i = \ddot{X} + \dot{u}_i \cos \theta_i - u_i \dot{\theta}_i \sin \theta_i - b \dot{\theta}_i^2 \cos \theta_i - b \ddot{\theta}_i \sin \theta_i$$
 (16)

$$\ddot{y}_i = \ddot{Y} + \dot{u}_i \sin \theta_i + u_i \dot{\theta}_i \cos \theta_i - b \dot{\theta}_i^2 \sin \theta_i + b \ddot{\theta}_i \cos \theta_i$$
 (17)  
By multiplying equation (11) by  $(-\sin \theta_i)$  and equation 12 by  $(\cos \theta_i)$  and using equations 16 and 17 we get

$$m(-2\ddot{X}\sin\theta_i + 2\ddot{Y}\cos\theta_i + u_i\dot{\theta}_i + b\ddot{\theta}_i) = \lambda_i. \tag{18}$$

By multiplying equation (11) by  $(\cos \theta_i)$  and equation (12) by  $(\sin \theta_i)$  and using equations (16) and (17) we get

$$m(2\ddot{X}\cos\theta_i + 2\ddot{Y}\sin\theta_i + \dot{u}_i - b\dot{\theta}_i^2) = -cu_i.$$
 (19)

Isolating  $\ddot{\theta}$  and then isolating  $\lambda_i$ , we have the reduced equations of motion of each Chaplygin sleigh,

$$\dot{u}_i = -\frac{c}{m}u_i + b\omega_i^2 - 2\ddot{X}\cos\theta_i - 2\ddot{Y}\sin\theta_i \qquad (20)$$

$$\dot{\omega_i} = \frac{-b\lambda_i - c_r\omega_i + \tau_i}{I} \tag{21}$$

$$\dot{\theta}_i = \omega_i \tag{22}$$

The equations of motion of the platform are

$$M\ddot{X} = \sum_{i=1}^{2} (2\lambda_i \sin \theta_i + cu_i \cos \theta_i) - 2KX$$
 (23)

$$M\ddot{Y} = \sum_{i=1}^{2} \left( -2\lambda_i \cos \theta_i + cu_i \sin \theta_i \right) - 2KY. \tag{24}$$

with the constraint (friction) forces that couple the motion of the platform to the two Chaplygin sleighs

$$\lambda_i = \frac{m(-2\ddot{X}\sin\theta_i + 2\ddot{Y}\cos\theta_i + u_i\dot{\theta}_i - \frac{\tau_i - c_r\dot{\theta}_i}{I})}{1 + \frac{mb^2}{I}} \quad (25)$$

The equations (14) and (15), that decoupled from the velocity equations, describe the evolution of the position of the Chaplying sleighs.

#### 3. SYNCHRONIZATION

We assume sinusoidal torques on the Chaplygin sleighs as

$$\tau_1 = B \sin(\Omega t + \phi_1)$$
 and  $\tau_2 = B \sin(\Omega t + \phi_2)$  (26)

where  $\Omega=\beta\sqrt{\frac{K}{M}}$ .  $\beta$  is the ratio of forcing frequency to the natural frequency of platform. The equations of motion (20)-(25) and (14)-(15) are numerically integrated using an explicit Runge-Kutta(4,5), Dormand-Prince solver in MATLAB. The results of such simulations presented here are based on the following parameters : for the Chaplygin sleigh m=1kg,  $I=1kgm^2$  and b=1m, for the platform M=1 kg and  $K=1\frac{N}{m}$ . The damping coefficients are set to  $c=1\frac{N.s}{m}$  and  $c_r=1\frac{N.m.s}{rad^2}$ . As the inputs to the system we set B=1 N.m and  $\beta=1$ . The results do not change for values of the frequency ratio  $\beta$  ranging from 0.8 to 2. The parameter that has a significant effect on the synchronization behavior is the phase difference  $\Delta\phi=\phi_2-\phi_2$  in the torques on the sleighs.

The initial velocity of the platform and the Chaplygin sleighs is assumed to be zero in all simulations and the initial orientations  $(\theta_i(0))$  are varied by selecting random numbers between  $[0\ 2\pi]$ . The platform is assumed to be initially motionless (X(0)=Y(0)=0). All simulations are done for a time duration of t=1000s (about 160 cycles of forcing) to ensure the velocities of the Chaplygin sleighs are close to the limit cycles, thus essentially identifying the limit cycles. Similar to the limit cycle solution  $(u(t),\omega(t))$  for a single Chaplygin sleigh moving on a fixed platform, the solutions  $(u_i(t),\omega_i(t))$  are periodic and appear as figure-8 limit cycles when projected onto the  $u_i-\omega_i$ . We will denote the average values  $\overline{u}_i=\lim_{T\to\infty}\frac{1}{T}\int_0^Tu_idt$ ,  $\overline{\omega}_i=\lim_{T\to\infty}\frac{1}{T}\int_0^Tu_idt$  and  $\overline{\theta}_i=\lim_{T\to\infty}\frac{1}{T}\int_0^T\theta_idt$ .

When  $\Delta \phi = 0$ , the average heading angles  $\overline{\theta}_1$  and  $\overline{\theta}_2$  differ by  $\pi$  as shown in the first row of fig. 3. Despite this the angular velocities  $\omega_i$  are equal and in phase (seen in the plot of  $\theta$  versus time) and the limit cycles (and hence  $u_i(t)$ ) are identical. In this case the two oscillators are

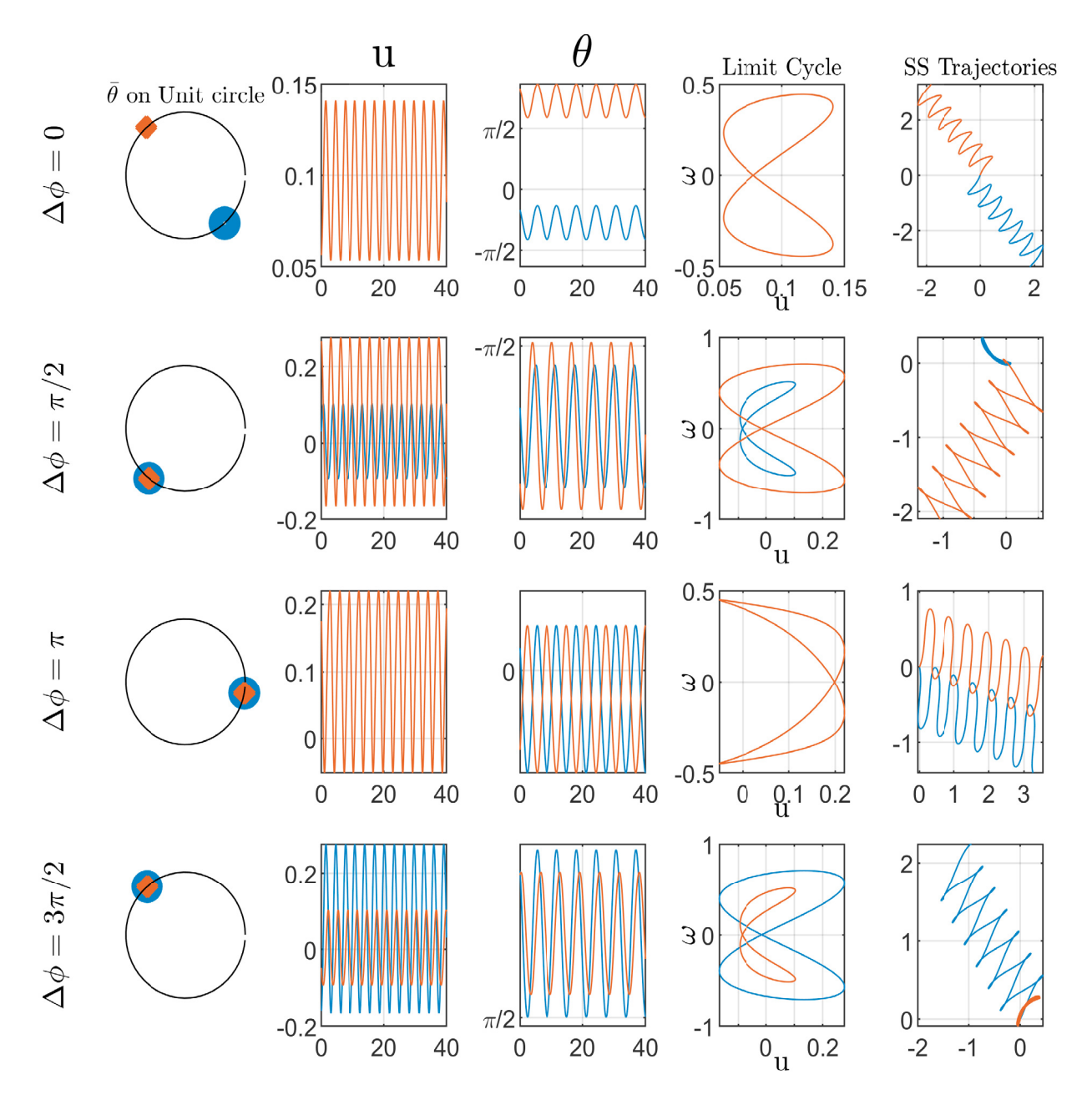


Fig. 3. Long time behavior of the coupled Chaplygin sleighs for four different values  $\Delta \phi$ . The two colors red and blue correspond to the variables of the two Chaplygin sleighs respectively. The first column shows the  $\bar{\theta}$  as a phase angle on the unit circle, the second and third columns shows the  $u_i(t)$  and  $\theta_i(t)$  and the fourth column shows the limit cycles in the  $(u_i - \omega_i)$  space. The fifth column is the steady state trajectory of the sleighs for the same period of time(40s).

synchronized in their phase, but anti-synchronized in their heading angle. As  $\Delta \phi$  increases to  $\frac{\pi}{2}$  the average angles  $\overline{\theta}_1$  and  $\overline{\theta}_2$  converge but the average speeds  $\overline{u}_1$  and  $\overline{u}_2$  are no longer identical as shown in the second row of fig. 3. The angular velocities  $\omega_i$  and the limit cycles are also no longer identical.

As  $\Delta \phi$  increases further, the limit cycles of the Chaplygin sleighs once again converge and become identical at  $\Delta \phi = \pi$ . The average heading angles  $\overline{\theta}_1$  and  $\overline{\theta}_2$  are also identical as seen in the third row of fig. 3. However the heading angle  $\theta_1$  and  $\theta_2$  are out of phase as seen in the plot of  $\theta$  vs time.

As  $\Delta\phi$  increases to  $\frac{3}{2}\pi$  the average angles  $\overline{\theta}_1$  and  $\overline{\theta}_2$  remain identical but  $\overline{u}_2$  and  $\overline{u}_1$  are no longer identical as shown in the last row of fig. 3. The angular velocities  $\omega_i$  and the limit cycles are also no longer identical. The rightmost column in fig. 3 shows the steady state trajectories of the Chaplygin sleighs. The steady state trajectories of the Chaplygin sleighs are anti-synchronized when  $\Delta\phi=0$  and synchronized in the average heading angle for the steady state trajectories when  $\Delta\phi=\pi$ . At  $\Delta\phi=\frac{\pi}{2}$  and  $\Delta\phi=\frac{3\pi}{2}$  one of the Chaplygin sleighs has a small speed and the steady state trajectory of the slower sleigh does not show a large displacement over time. In fact the the slower sleigh's

motion is bounded in the numerical simulations. The steady state trajectories  $(x_i(t),y_i(t))$  shown in fig. 3 were obtained by shifting (translating) the trajectories back to the origin for comparison. Figure 4 shows a schematic of the two Chaplygin sleighs overlaid on the steady state trajectories and the phase on the limit cycles.

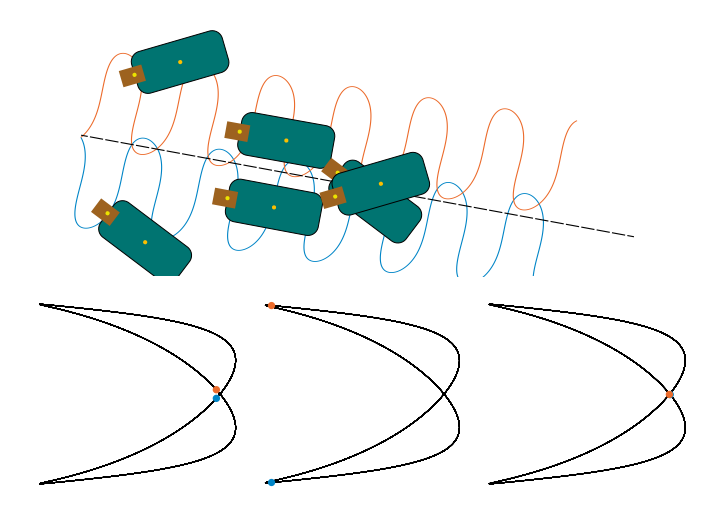


Fig. 4. Anti-phase synchronization of  $\theta_i(t)$  leads to identical limit cycles and the same average heading angle  $\overline{\theta}$ .

The dependence of the synchronization and anti-phase synchronization of the average heading angles  $\theta$  is found to be almost the same for a large set of initial angles  $\theta_1(0)$ and  $\theta_2(0)$ . Figure 5(a) shows the  $\overline{\theta}_1 - \overline{\theta}_2$  as a function of  $\Delta \phi$  for 20 randomly chosen initial angles. For all the initial angles of the Chaplygin sleighs the average heading angles are synchronized for  $\Delta \phi \in [0, \frac{\pi}{2} - \epsilon]$  and  $\Delta \phi \in [\frac{3\pi}{2} + \epsilon]$  $\epsilon, 2\pi$  where numerical simulations show that  $\epsilon < 0.045$ . Similarly the dependence in the difference of the average speeds of the Chaplygin sleighs is found to be almost the same for a large set of initial angles  $\theta_1(0)$  and  $\theta_2(0)$ . Figure 5(b) shows the  $\overline{u}_1 - \overline{u}_2$  versus  $\Delta \phi$ . This graph of this difference has the shape of a half cosine function; it is zero at  $\Delta \phi = 0$  and decreases until  $\Delta \phi = \pi/2$ . Then we see step increase at this point and decreases as a cosine function until falls to zero again at  $\Delta \phi = \pi$ .

Most interestingly when the angles  $\theta_1$  and  $\theta_2$  are antiphase synchronized, the mean values of  $\theta_1(t)$  and  $\theta_2(t)$  converge to the mean of the initial angles  $\theta_1(0)$  and  $\theta_2(0)$  when  $\Delta \phi = \pi$  as shown in fig. 6(a). This behavior persists across different randomly chosen initial conditions.

The motion of the Chaplying sleighs on the platform have an interesting relation to the motion of the platform itself. Figure 7 shows the steady state motion (X(t),Y(t)) of the plate. In the top row the amplitude is negligibly small when  $\Delta\phi=0$  and grows when the Chaplygin sleighs are not synchronized in either the angle nor the limit cycles. When  $\Delta\phi=\frac{\pi}{2}$  or  $\Delta\phi=\frac{3\pi}{2}$  the limit cycles of the sleighs differ significantly with the speed of one of the sleighs being smaller than that of the other. The slower sleigh does not move significantly and its motion is bounded upto numerical accuracy. In such cases the oscillations of the platform are larger. When the sleighs' motion is antiphase synchronized and they move with identical speeds

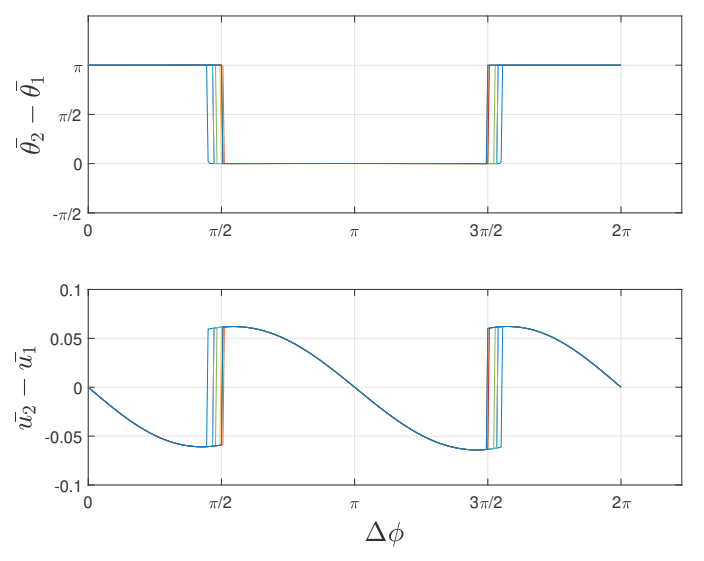


Fig. 5. (a)  $\overline{\theta}_1 - \overline{\theta}_2$  as a function of  $\Delta \phi$  and (b)  $\overline{u}_1 - \overline{u}_2$  as a function of  $\Delta \phi$  for 20 different randomly chosen initial conditions.

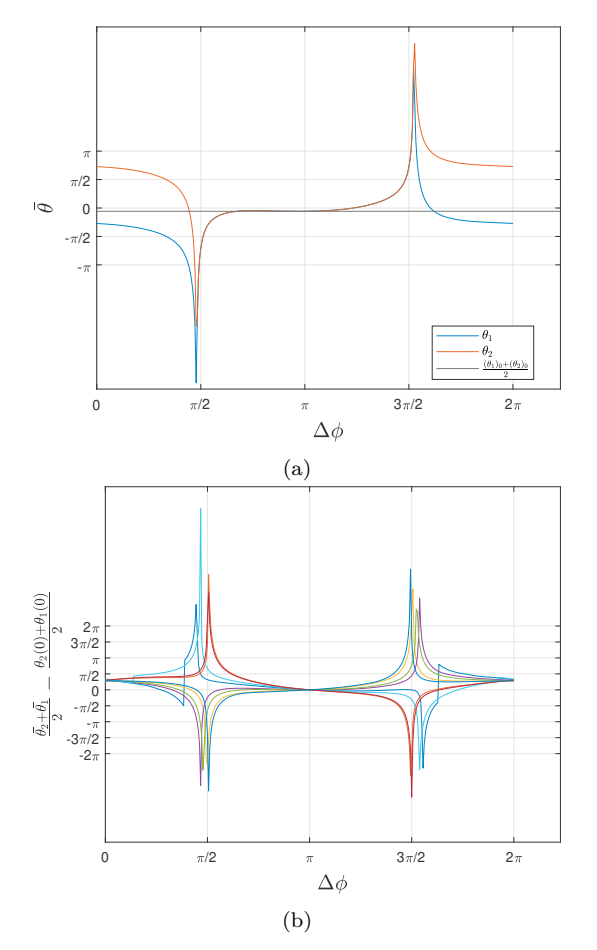


Fig. 6. (a) Blue is  $\overline{\theta}_1$  and red is  $\overline{\theta}_2$ . Both converge to  $\frac{1}{2}(\theta_1(0) + \theta_2(0))$  when  $\Delta \phi = \pi$ . (b)A plot of  $\frac{1}{2}(\overline{\theta}_1 + \overline{\theta}_2) - \frac{1}{2}(\theta_1(0) + \theta_2(0))$ . The average heading of the Chaplygin sleighs converges to the mean of the initial angles when  $\Delta \phi = \pi$  for 20 randomly chosen initial angles

in the same direction, the amplitude of the oscillations of the platform is smaller. This decrease can be attributed to the anti-phase of the angles  $\theta_1$  and  $\theta_2$ . This results in the friction force exerted between each sleigh and the platform to oppose each other for one half of the cycle along a limit cycle.

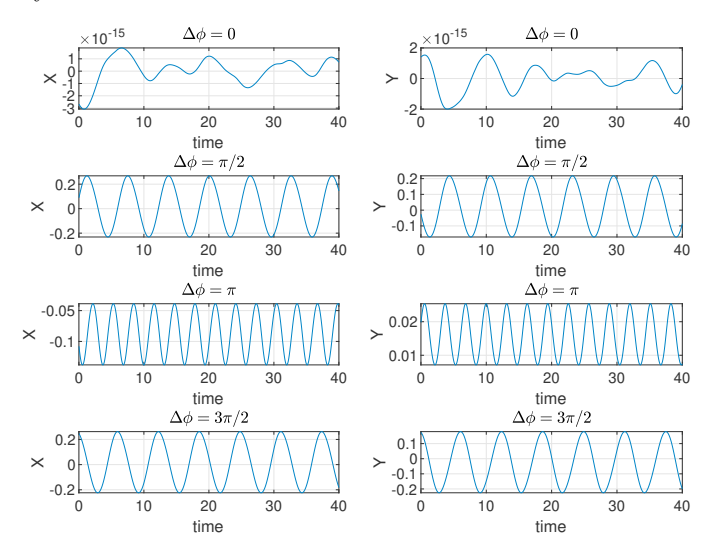


Fig. 7. Steady state oscillations of the platform for different  $\Delta \phi$ . In the top row, the amplitude is negligibly small when  $\Delta \phi = 0$ .

#### 4. CONCLUSION

This paper describes a novel problem of the synchronization of a pair of mobile coupled nonholonomic oscillators. The coupling of the motion is via a movable plate. When the actuation for the oscillators are out of phase, it is shown that the average angle of the oscillators are also out of phase. In this anti-phase synchronization, the nonholonomic systems move in the same direction at the same speed. During such anti-phase synchronization, the plate's motion is of smaller amplitude. In contrast, when the oscillators are not synchronized, the motion of the plate has a higher amplitude. This novel problem and the results of the synchronized motion in 'formation' and conditions leading to such a phenomenon can have important applications in mobile robotics.

## REFERENCES

Bennett, M., Schatz, M.F., Rockwood, H., and Wiesenfeld, K. (2002). Huygens's clocks. *Philosophical Transactions of the Royal Society*, 458, 563–579.

Bialek, W., Cavagna, A., Giardina, I., M., T., Silvestri, E., Viale, M., and Walczak, A.M. (2012). Statistical mechanics for natural flocks of birds. *Proceedings of the* National Academy of Science, 13(109), 4786–4791.

Borisov, A.V. and Mamaev, I.S. (2009). The dynamics of a chaplygin sleigh. *Journal of Applied Mathematics and Mechanics*, 73(2), 156–161.

Buchanan, B., Travers, M., Choset, H., and Kelly, S. (2020). Stability and control of chaplygin beanies coupled to a platform through nonholonomic constraints. In *Dynamic Systems and Control Conference*, V002T30A006.

Buhl, J., Sumpter, D.J.T., Couzin, I.D., Hale, J.J., Despland, E., Miller, E.R., and Simpson, S.J. (2006).

From disorder to order in marching locusts. *Science*, 312(5778), 1402–1406.

Fedonyuk, V. and Tallapragada, P. (2018). Sinusoidal control and limit cycle analysis of the dissipative chaplygin sleigh. *Nonlinear Dynamics*.

Free, B.A., Lee, J., and Paley, D.A. (2020). Bioinspired pursuit with a swimming robot using feedback control of an internal rotor. *Bioinspiration and Biomimetics*, 15(3), 035005.

Ghanem, P., Wolek, A., and Paley, D.A. (2020). Planar formation control of a school of robotic fish. In 2020 American Control Conference (ACC), 1653–1658.

Herbert-Read, J.E. (2016). Understanding how animal groups achieve coordinated movement. *Journal of Experimental Biology*, 219(19), 2971–2983.

Huygens, C. (1669). Instructions concerning the use of pendulum-watches, for finding the longitude at sea. Philosophical Transactions of the Royal Society, 4, 937– 953.

Kuramoto, Y. (1975). Self-entrainment of a population of coupled non-linear oscillators. In *International Symposium on Mathematical Problems in Theoretical Physics*, 420–422. Springer Berlin Heidelberg.

Lee, J., Free, B., Santana, S., and Paley, D.A. (2019). State-feedback control of an internal rotor for propelling and steering a flexible fish-inspired underwater vehicle. In 2019 American Control Conference (ACC), 2011–2016.

Neimark, J.I. and Fufaev, N.A. (1972). Dynamics of nonholonomic systems. AMS.

Paley, D.A., Thompson, A.A., Wolek, A., and Ghanem, P. (2021).
Planar formation control of a school of robotic fish: Theory and experiments. Frontiers in Control Engineering, 2.

Pikovsky, A., Rosenblum, M., and Kurths, J. (2001). Synchronization, a universal concept in nonlinear sciences. 2, 3.

Pollard, B. and Tallapragada, P. (2017). An aquatic robot propelled by an internal rotor. *IEEE/ASME Transaction on Mechatronics*, 22(2), 931–939.

Pollard, B. and Tallapragada, P. (2019). Passive appendages improve the maneuverability of fish-like robots. *IEEE/ASME Transactions on Mechatronics*, 24(4), 1586–1596.

Strogatz, S. (2003). Sync–the emerging science of spontaneous order, trad. it.

Willms, A.R., Kitanov, P.M., and Langford, W.F. (2017). Huygens' clocks revisited. *Philosophical Transactions of the Royal Society*, 4, 170777.

Winfree, A.T. (1967). Biological rhythms and the behavior of populations of coupled oscillators. *Journal of Theoretical Biology*, 16(1), 15–42.